Modeling of Interaction of Electromagnetic Fields from a Cellular Telephone with Hearing Aids

Michal Okoniewski, *Senior Member, IEEE*, and Maria A. Stuchly, *Fellow, IEEE*

***Abstract*—The new generation of cellular telephones and other personal communication services (PCS's) poses new problems and challenges in interactions with the human body. Among them is electromagnetic interference (EMI) with medical devices, particularly for systems using time-division multiple access (TDMA). Hearing aids are among the devices affected by the pulse modulation in the audio range associated with the TDMA systems. While EMI in this case does not generally pose a health risk, it constitutes a considerable annoyance, which may prevent the hearing-aid wearers from using some of the new communication devices. Also, just the proximity to the devices used by others or the base station may result in signals sufficient to interfere with proper perception of sounds. We have evaluated the electric and magnetic fields in the ear canal at 900 MHz for a typical monopole antenna on a typical handset, an equivalent dipole, and a plane wave. Special care was taken to properly represent the anatomy of the ear, including its canal. The finite-difference time-domain (FDTD) method was used to compute the electric and magnetic fields in the ear canal and around the ear. The fields from the exposure sources in various realistic placements of the hearing aid were compared. The results presented are of importance and use in developing performance standards and practical testing methods for various types of hearing aids.**

***Index Terms*— Cellular telephone, EMI, FDTD, hearing aids, wireless communication.**

I. Introduction

THE new generation of cellular telephones and other personal communication services (PCS's), as well as a global system for mobile communication (GSM), poses new problems and challenges in interactions with the human body and medical devices. One type of device affected are hearing aids. It has been reported [1]–[3] that electronmagnetic interference (EMI) in hearing aids is associated with the frame rate in time-division multiple-access (TDMA) systems, resulting in the pulse modulation of the RF signal in the audible range. The frequency of the pulses depends on the communication system, and is typically 50 Hz or 217 Hz for TDMA systems. For code-division multiple-access (CDMA) systems, interference may also result due to the voice encoder/decoder and automatic adjustment of the output power [2], [3]. While the EMI in these cases does not generally pose a health risk, it constitutes a considerable annoyance, which may prevent the hearing-aid wearers from using some of the new devices. The proximity to cellular telephones used by others or the base station may also result in sufficiently strong signals to interfere with proper perception of sounds. Evaluation of EMI has been done experimentally, and protocols for testing are being developed, e.g., at the Center for Devices and Radiological Health, FDA, Rockville, MD [2], [3]. There are three typical locations of hearing aids:

1) behind the ear;
2) at the entrance to the ear canal;
3) deeper inside the ear canal.

The actual placement depends on the hearing-aid size and the user's ear. The pickup of RF originals is by a small coil in the piezoelectric transducer. The coil is not shielded. The experimental test procedures can be greatly simplified if the levels of the electric and magnetic fields around and in the ear at various locations where hearing aids are typically located are known for actual complex exposure situations. The complexity results from the perturbation by the human head of the electric and magnetic fields from cellular telephones or their equivalent representation. To evaluate the actual potential for EMI, the assessment of the fields has to be made behind the ear and inside the ear canal. Simplified testing of actual hearing aids performed in free space using a resonant dipole representing a cellular telephone [2], [3] can then be related to the practical complex fields. Similarly, it is important for testing and evaluation purposes to consider a plane-wave exposure, which simulates the situations for the base stations and a cellular telephone at a sufficiently large distance.

The finite-difference time-domain (FDTD) method has proven to be a method of choice in modeling the interactions of RF fields from cellular telephones with the human head (e.g., [4]–[6]), as it can easily accommodate a heterogeneous electrical model of the human head and allow for high resolution of computations of the electric and magnetic fields. Therefore, we have selected the FDTD to model the EMI with hearing aids. A current transformer (CT) and MRI-derived high-resolution model of the human head is used. Fields are computed for a generic cellular telephone, an equivalent resonant dipole, and an uniform plane wave. Modeling is performed at a frequency of 900 MHz. All results are normalized to 1 W of the antenna output power for the cellular telephone and dipole, and to 1 V/m for the plane wave.

II. Models and Method of Analysis

An anatomically correct model of the human head comprising some 20 tissues was used. The head model was based on the image segmentation of the CT and MRI scans [7] with additional manual corrections of the reconstructed anatomy as

Manuscript received October 29, 1997; revised April 2, 1998. This work was supported under a Contract from Bell Mobility, under a Contract from Rogers Cantel, and under a Grant from NSERC-CRD.

The authors are with Department of Electrical and Computer Engineering, University of Victoria, Victoria, B.C., Canada V8W 3P6.

Publisher Item Identifier S 0018-9480(98)08001-6.

required. The model resolution was 1.1 mm × 1.1 mm in the horizontal plane, and 1.4 mm in the vertical plane. The tissue properties were selected as in [4].

Particular attention was paid to the correctness of the anatomy of the outer and inner ear. For the modeling of the fields in the ear canal, we developed a guiding tool (the so-called "electronic worm") that allowed us to automatically find locations in the center of the ear canal. This was essential, as otherwise it would have been tedious and unreliable to find the points at which the fields were relevant to the problem investigated. The electronic worm was developed using a visualization program Data Explorer (IBM). The tool consists of a tube with protrusions normal to its surface. The protrusions are straight and spaced at varying separations. Both the tube and protrusions change color depending on the tissue. In the case of the tube, tissue inside it is of interest, while for the protrusions (tentacles), it is the tissue they touch with their free ends. The worm is shown in Fig. 1(a), where the dark grey color indicates air and the pale grey indicates other tissues. Placement of the final smaller diameter tube obtained by means of the electronic worm is shown in Fig. 1(b). This tube is smaller in diameter (3 mm), and the results of the computations are automatically mapped on to the tube.

The FDTD method was used for the analysis because of its flexibility and efficiency in solving complex heterogeneous geometries. The Yee-cell rectangular computational grid [8] and the scattered and total field formulation [9] were used. The computational space was truncated by a perfectly matched layer (PML) of seven-cell thickness with a parabolic profile to ensure reflections below at least 40 dB [10]. The total computational space was 350 × 320 × 340 mm (without the PML), and was meshed with $dx = dy = 3.4$ mm (horizontal plane) and $dz = 4.7$ mm, except for the volume surrounding the ear and antenna. In that area of 70 × 145 × 140 mm, the subgridding algorithm was used, which reduced the spatial and time steps by a factor of two [11]. Computations were performed with continuous-wave (CW) excitation, and typically 1250–1300 iterations were required; the stability margin was 0.72, as required by the subgridding algorithm [11].

Since the original head model had a different resolution from the computational grid, an automatic remeshing algorithm was used, which was based on the field-continuity conditions and integral form of Maxwell's equations in a subcell regime. Using fast logical integration and the flux-weighted averages, look-up tables of the dielectric constant and conductivity were assembled for each field component separately. This algorithm increased the accuracy of computations. Computations were performed on a Hewlett-Packard workstation HP9000/735.

The cellular telephone was represented by a metallic box of 30 × 60 × 140 mm, covered with 2-mm dielectric of a relative dielectric constant of 2. The monopole was centrally located on the box and was 85-mm long. The dipole was 160-mm long. Both antennas were excited in the gap one-grid wide with a source having 50-Ω impedance. In the case of the cellular telephone, the earpiece was aligned with the ear canal, and at a minimal distance from the ear. This placement resulted in the monopole gap being positioned above the ear. The dipole was placed at the same distance from the ear as the monopole.

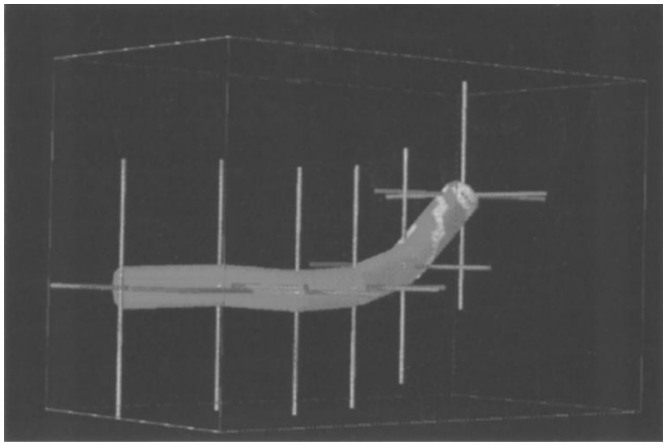

(a)

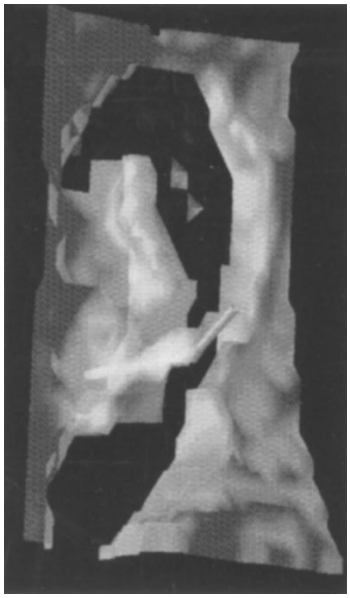

(b)

Fig. 1. Tools for identification of the ear canal. (a) The "electronic worm" with its tentacles that change color depending on the tissue they touch. (b) A view of a 3-mm-diameter tube through the ear canal. The electric and magnetic fields are computed along and in the center of this tube.

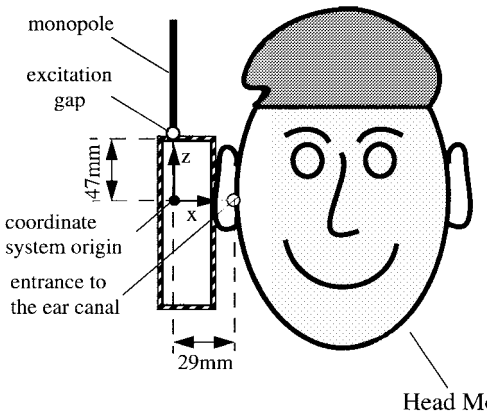

Fig. 2. Position of the handset and ear with respect to the coordinate system.

Two positions of the gap with respect to the entrance to the ear canal were considered: the gap in the same location as the gap in the monopole on the handset and the gap

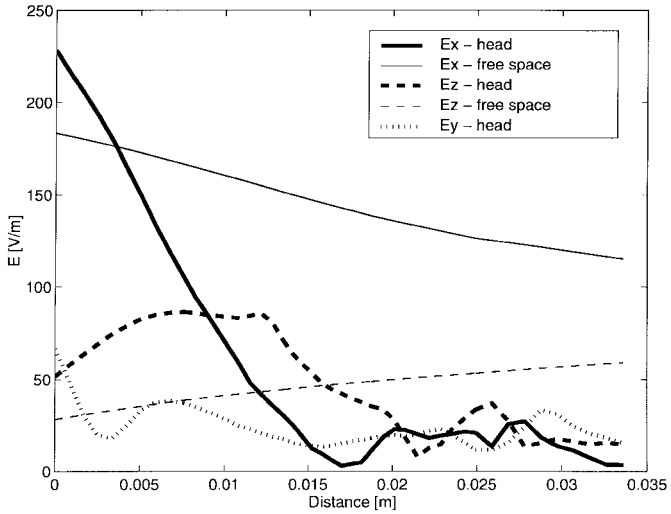

(a)

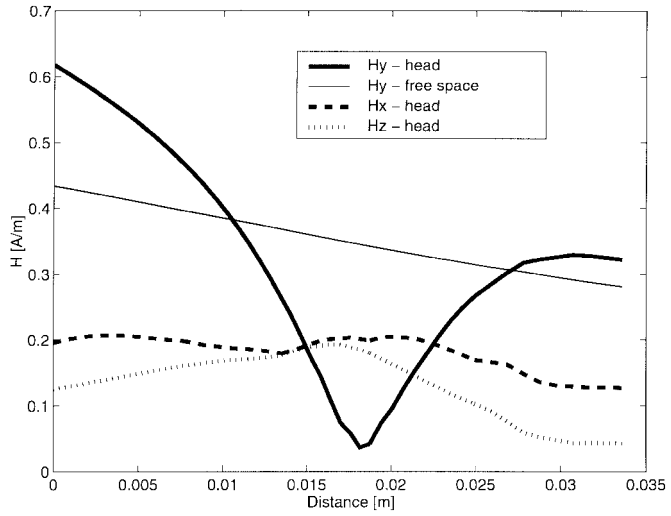

(b)

Fig. 3. Monopole on the handset. (a) The electric fields and (b) magnetic fields in the ear canal and free space without the head. Antenna output power 1 W at 900 MHz. Distance $= 0$ corresponds to the entrance to the ear canal ($x = 29$ mm, $z = 0$). Note that x, y, z vary as the distance increases (the ear canal is not aligned with any of the coordinate axis).

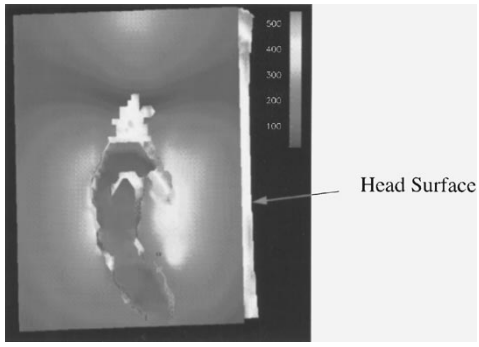

(a)

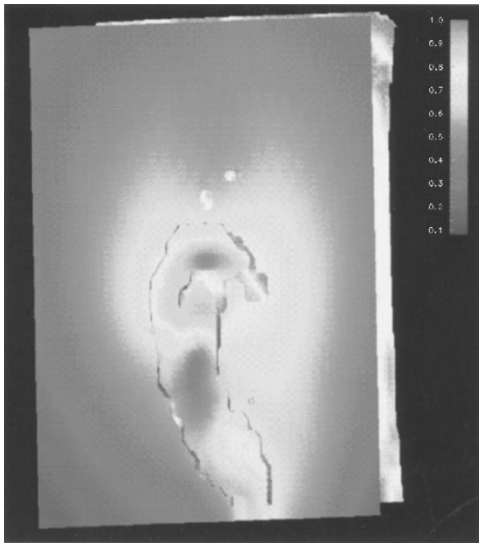

(b)

Fig. 4. Exposure to the monopole on the handset with the excitation gap placed at $x = 0$ (as shown in Fig. 2) and $z = 47$ mm. Patterns of the fields in the plane parallel to the entrance to the ear canal and about 5 mm from the head (i.e., in the plane $x = 24$ mm). (a) The magnitude of the electric field (V/m). (b) The magnitude of the magnetic field (A/m).

aligned with the entrance to the ear canal. Both antennas were always in the vertical position. The origin of the coordinate system was placed in the intersection of the axis of the ear canal with the axis of the antenna. The coordinate system axes are as follows: x horizontal toward the head, z vertical pointing up. Fig. 2 illustrates the placements of the cellular telephone and the entrance to the ear canal with respect to the coordinate system. In the case of the plane wave, the wave was incident normally to the plane of the entrance to the ear canal (i.e., propagating in x-direction) with the electric field in z-direction. It is emphasized that the whole length of the ear canal is not aligned with any of the coordinate system axis.

III. Results of Modeling

A. Cellular Telephone

Fig. 3 illustrates the electric and magnetic fields in the ear canal for a monopole antenna on the handset at 900 MHz and antenna output power of 1 W. The handset is placed as close to the ear as possible, with the ear piece in contact with the ear, and the handset in a vertical position. It should be noted that the vertical position of the handset results in the maximum absorption of the radiated power in the head [6]. In Fig. 3, zero distance shown on the abscissa refers to $x = 29$ mm and corresponds to the entrance of the ear canal. The distance is measured inside the ear canal, which is not aligned with any axis of the coordinate system. This distant is measured by means of the electronic worm. As shown in Fig. 3(a), the electric field E_x dominates over E_z in free space. The E_x decreases and E_z increases as the distance from the handset increases. This behavior of the fields is consistent with the known relationships for the electric field of a dipole in the near field [12]. Since the metallic part of the handset can be considered as the second arm of the dipole, the use of the dipole-field expressions rather than of the monopole is justified [13]. The head in the close proximity of the cellular-telephone antenna, as expected, perturbs both components of the electric field and excites an additional electric-field component (E_y). This is consistent with the previously published data [4]–[6]. Overall, the field strength

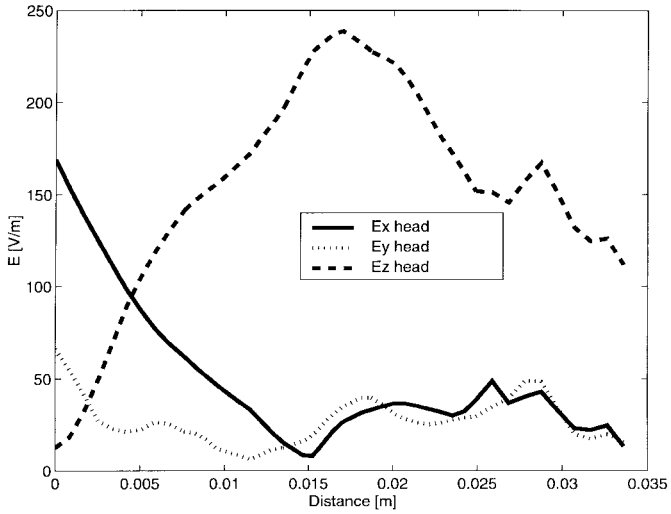

(a)

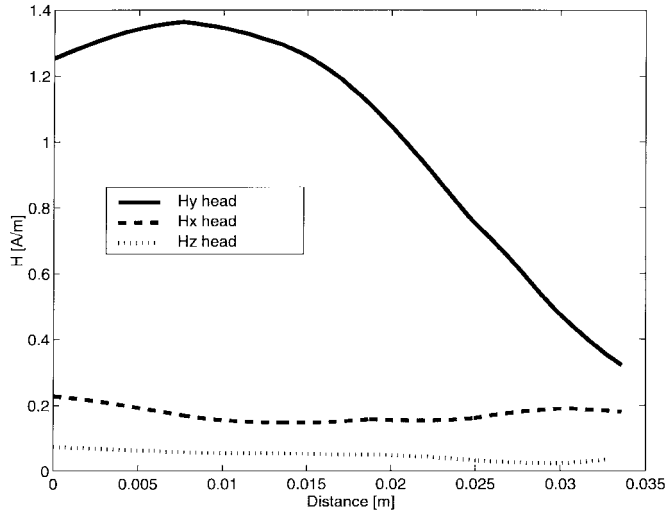

(b)

Fig. 5. Dipole with the excitation gap in the same position as the excitation gap of the monopole. (a) The magnitude of the electric field. (b) The magnitude of the magnetic field in the ear canal. Antenna output power 1 W at 900 MHz.

decreases with distance away from the ear-canal entrance for the dominant component (E_x).

The behavior of the magnetic field is shown in Fig. 3(b). In free space, H_y is the only component of the magnetic field present [12] and, similarly to the electric field, the head in close proximity interacts with the antenna and produces two additional, though weaker, components of the magnetic field. The strength of the magnetic field (as well as the electric) is greater at the entrance (distance $= 0$) to the ear canal than in the same location in free space for the same antenna output power. This behavior is reasonable and expected because of the high dielectric constant and conductivity of the tissues in the head [4]. The dominant component of the magnetic field exhibits a standing-wave pattern in the ear canal with the null located approximately a quarter-wave from the ear-canal wall. This may be explained by high conductivity of the cerebrospinal fluid located just behind that wall.

To further illustrate the complex nature of fields, maps of the electric-field [see Fig. 4(a)] and magnetic-field [see Fig. 4(b)]

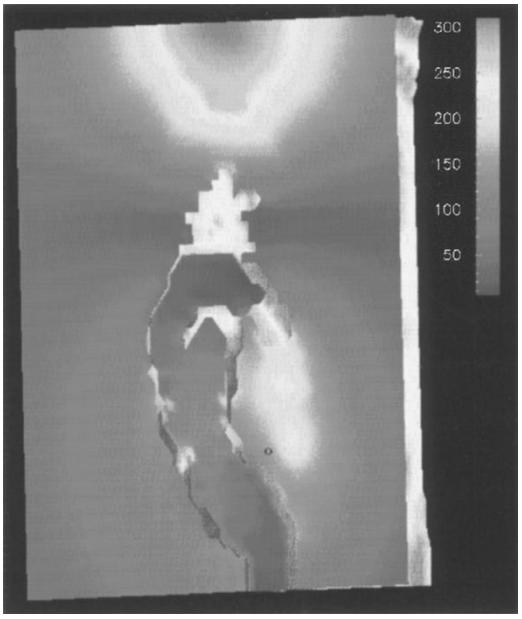

(a)

(b)

Fig. 6. Exposure to the dipole placed in the monopole position. Patterns of the fields in the plane parallel to the entrance of the ear canal and about 5 mm from the head (i.e., in the plane $x = 24$ mm). (a) The magnitude of the electric field (V/m). (b) The magnitude of the magnetic field (A/m).

intensity around the ear are given in the plane normal to the ear canal axis and just in front (5 mm) of the ear-canal entrance. This plane cuts through that part of the ear where the hearing aids are normally placed. The outline demarcates the ear location. Strong magnetic fields can be noticed close to the upper part of the ear. That part is very close to the excitation gap.

Additional computations were also performed for positions of the handset separated by greater distances from the head.

B. Dipole

Fig. 5 shows the electric and magnetic fields for the dipole with the gap in the same place as the monopole gap. The

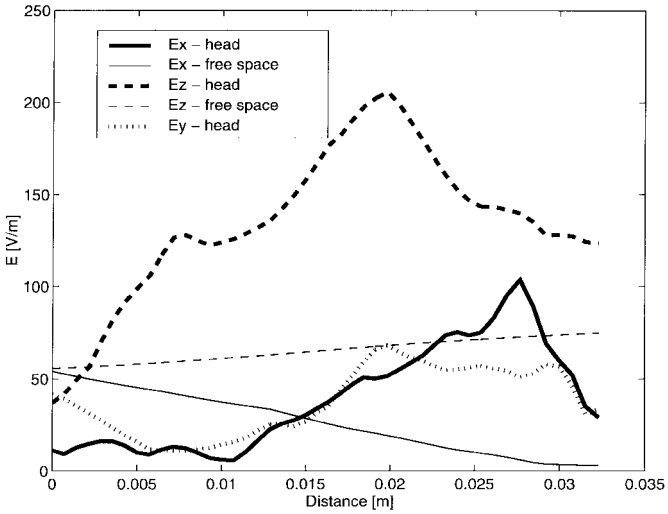

(a)

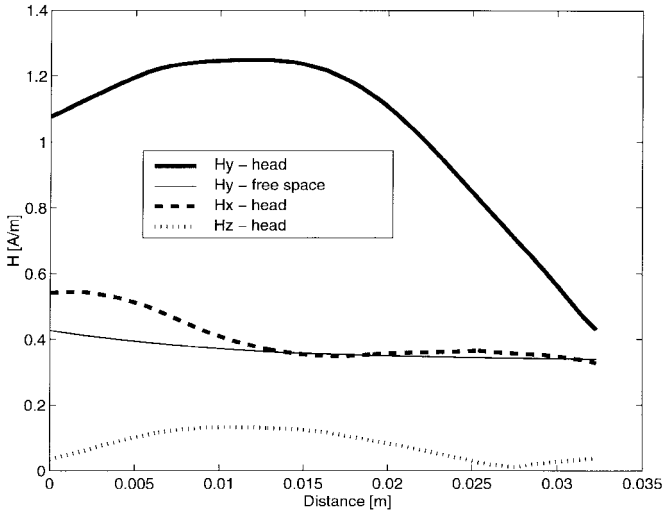

(b)

Fig. 7. Dipole with the excitation gap aligned with the ear canal. (a) The magnitude of the electric field. (b) The magnitude of the magnetic field in the ear canal. Antenna output power 1 W at 900 MHz.

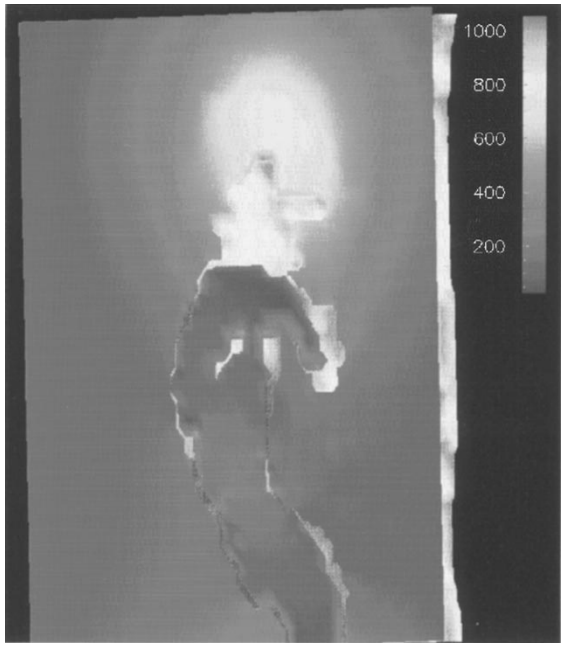

(a)

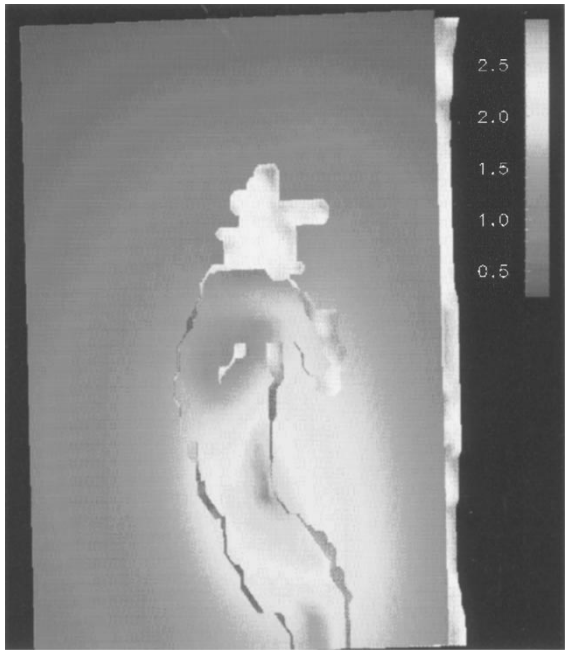

(b)

Fig. 8. Exposure to the dipole with the excitation gap aligned with the ear canal. Patterns of the fields in the plane parallel to the entrance of the ear canal and about 5 mm from the head (i.e., in the plane $x = 24$ mm). (a) The magnitude of the electric field. (b) The magnitude of the magnetic field.

fields in free space are very similar or nearly identical to those shown in Fig. 3 because of the handset metallic box acting as one arm of the dipole (and the monopole as the other). Contrary to the monopole, the dominant component of the electric field is E_z (vertical) rather than E_x. The difference relates to the fact that the handset, which constitutes a part of the antenna, is practically in contact with the ear (the handset is covered with a thin lossless dielectric material). As a result, also in the ear canal, the dominant components of the electric field are different for the monopole and dipole. However, the magnetic fields have the same components in the ear canal for the monopole on the handset and dipole. The magnitude of the dominant component of the magnetic field is substantially higher in the case of the dipole.

To further illustrate the field distributions, Fig. 6 shows the field maps in the plane 5 mm in the front of the ear canal and parallel to the entrance of the ear canal. The electric-field pattern in this plane is not much different from that for the monopole (see Fig. 4). The maximum magnetic field is shifted toward the ear center and toward the ear canal, as shown in Fig. 6(b).

Modeling of the fields in free space for the dipole was verified against the analytical solution [12], and an excellent agreement was obtained (within 5%).

In testing for EMI of cellular telephones with hearing aids, the dipole is frequently placed with its excitation gap aligned with the ear canal (or the hearing aid). Fig. 7 illustrates the fields in the ear canal for this placement of the dipole. The field components in the same positions, but in free space, are

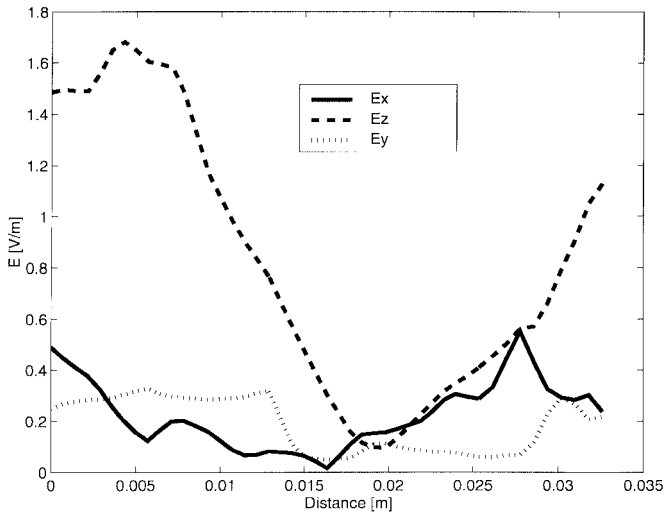

(a)

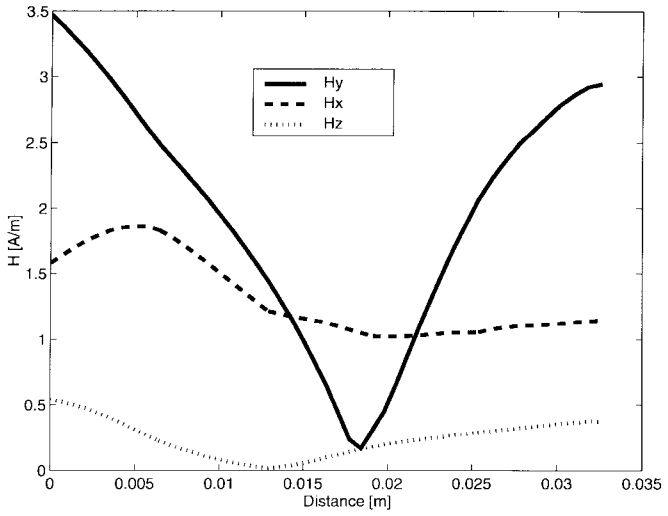

(b)

Fig. 9. Exposure to the plane wave propagating in x-direction (toward the ear) with the electric field in z-direction. (a) The electric fields normalized to 1 V/m in the reference plane corresponding to "distance = 0" (just in front of the ear canal) in free space. (b) Magnetic fields normalized to the free space magnetic field H_o.

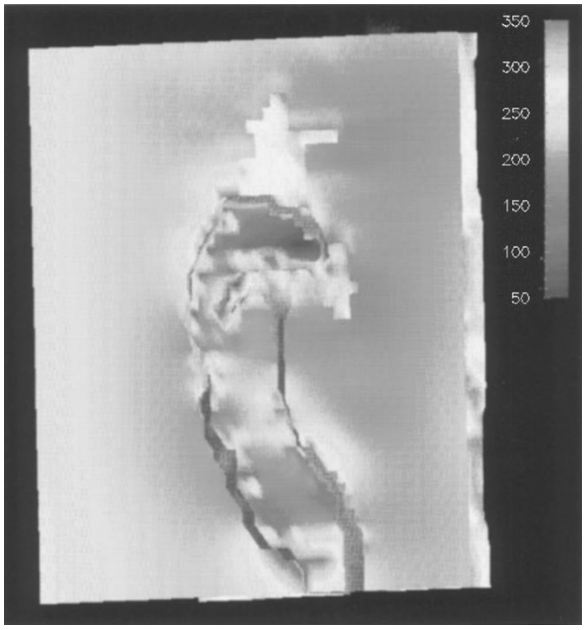

(a)

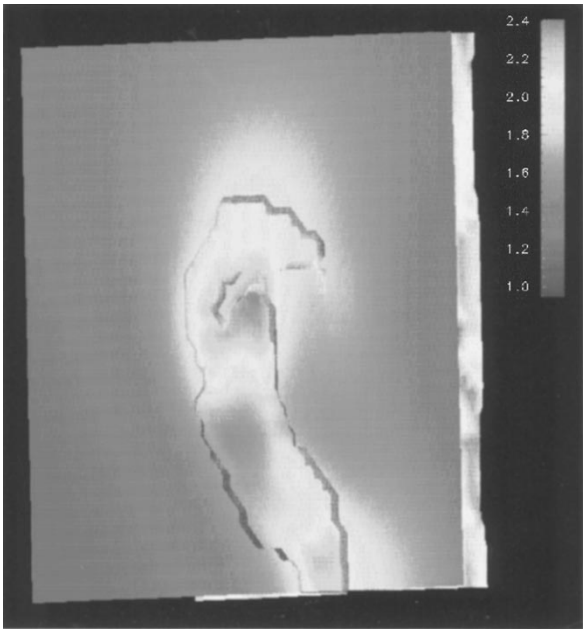

(b)

Fig. 10. Exposure to the plane wave. Pattern of the electric fields in the plane parallel to the entrance to the ear canal located at $x = 24$ mm. (a) The magnitude of the electric field (V/m). (b) The magnitude of the magnetic field (A/m).

also shown. The patterns of E_z and E_y are quite similar for the two placements of the dipole [see Figs. 7(a) and 5(a)]. It can also be noted by comparing the free-space magnitudes of E_z for the two dipole locations [see Figs. 5(a) and 7(a)] that they are similar and, thus, are approximately the magnitudes of these fields in the ear canal. The behavior is vastly different for E_x. Firstly, in free space, the magnitude of this field for the dipole with the excitation gap aligned with the ear canal [see Fig. 7(a)] is less than one-third of that with the dipole with the excitation gap in the same position as the handset gap [see Fig. 5(a)]. Consequently, E_x in the ear canal has a very different pattern for the two placements of the dipole [see Figs. 5(a) and 7(a)].

There are much smaller differences between the magnetic-field patterns for the two placements of the dipole [see Figs. 5(b) and 7(b)]. Further illustration of the behavior of both the electric and magnetic field is provided in Fig. 8. For the electric field, the differences in the field maps are apparent when the maps in Figs. 6(a) and 8(a) are compared. The similar behavior of the magnetic fields in the ear canal corresponds to the very similar magnetic-field maps at the entrance to the ear canal, shown in Figs. 6(b) and 8(b).

C. Plane Wave

As the last test, the behavior of a plane wave incident from x-direction with E_z and H_y is illustrated in Fig. 9. The magnitude of E_z is 1 V/m in free space anywhere. Similarly,

TABLE I
COMPARISON OF FIELD MAGNITUDES FOR DIFFERENT HEARING-AID PLACEMENT AND THREE EXPOSURE SOURCES

Exposure	Behind the ear		Entrance to the ear canal		1 cm in the canal		Maximum in the canal	
	|E| (V/m)	|H| (A/m)	|E| (V/m)	|H| (A/m)	|E| (V/m)	|H| (A/m)	|E| (V/m)	|H| (A/m)
Telephone 1 W x = 29 mm	230	0.64	241	0.66	110	0.48	241	0.66
Telephone 1 W x = 39 mm	180	0.5	175	0.50	70	0.34	175	0.50
Telephone 1 W x = 49 mm	155	0.45	150	0.43	60	0.29	150	0.43
Dipole 1 W x = 29 mm z = 47 mm	174	0.82	180	1.27	165	1.37	240	1.4
Dipole 1 W x = 69 mm z = 47 mm	93	0.44	72	0.35	20	0.2	72	0.35
Dipole 1 W x = 29 mm z = 0 mm	168	2.8	57	1.2	125	1.3	210	1.3
Plane wave	242	1.86	245	1.65	80	1.1	245	1.65

as for the monopole and dipole, there are components of the electric [see Fig. 9(a)] and magnetic fields [see Fig. 9(b)] in the ear canal that are not present in the plane wave. The strengths of both fields are also greater at the entrance to the ear canal than those in free space. The fields in the canal in many positions are stronger than in the plane wave (greater than 1 V/m). This may appear surprising, but is plausible, as tissues have high dielectric constant and are quite conductive. Fig. 10 shows the patterns of the electric and magnetic field close to the ear-canal entrance for the plane wave. The differences in the field maps for the plane wave and dipoles and handset are quite pronounced.

IV. COMPARISON OF VARIOUS EXPOSURES

To facilitate the comparison of the considerable amount of data obtained in the modeling of fields in the ear canal and around the ear, Table I gives the field strengths in three specified locations and in the locations of the maximum field magnitude (these vary, as shown in Figs. 3, 5, 7, and 9) for various exposures. These locations are selected to represent typical and the possible "worst case" placements of the hearing aids. For the plane-wave exposure shown in Table I, it is assumed that the H_y was equal to that produced by the 1-W handset antenna in free space. This results in the normalization factor for the magnetic fields of 0.43 and for the electric fields of 162 ($0.43 \times 120\pi$).

One apparent observation is that the field patterns and magnitudes for the three sources of exposure are quite different. Overall behavior is complex, but certain general features can be identified. In the case of the monopole antenna, fields at points behind the earlobe have similar magnitude as at the ear-canal entrance. For the dipole with a gap aligned with the ear canal, or shifted upwards from the ear, the electric fields are lower than for the monopole. Inside the ear canal at 1-cm depth, both dipoles produce stronger fields. However, the dipole produces significantly higher magnetic fields for both placements considered. As the dipole is shifted away from the ear, its field pattern becomes similar to that of the plane-wave exposure. The monotonic decrease in both fields with an increase in distance of the antenna from the head is expected, and this result increases confidence in the modeling results. The fields in the ear canal are generally attenuated; however, standing-wave-like behavior of some field components is also present.

V. CONCLUSIONS

Realistic modeling of the electric and magnetic fields to which hearing aids are subjected due to cellular telephones and other sources has been performed. A CT and MRI-based anatomically realistic model of the human head with a well-defined ear canal has been utilized. Field simulations have been performed at 900 MHz using the FDTD method. The geometry

and exposure source selection have been influenced by the ongoing experimental investigations of EMI for hearing aids.

The electric and magnetic fields for all exposure conditions are significantly different in the ear canal and other locations where a hearing aid may be placed when evaluated with the human-head model from those calculated for the same transmitter in free space. This indicates that evaluation of EMI from cellular telephones and other wireless communication devices with hearing aids should take into account the field perturbation by the human body. Our computations have also showed that a dipole is not an adequate representation of a cellular telephone with a monopole antenna at 900 MHz. On the other hand, we anticipate that the data presented can help in setting reliable and simplified experimental test procedures for EMI evaluation of hearing aids. We have also found that for cellular telephones that are further away, e.g., used by another person, a dipole remotely located or a plane wave both constitute reasonable equivalent (to the handset) sources for EMI evaluation. Finally, our modeling results need to be compared with the experimental data to fully explore their value in EMI testing of hearing aids.

ACKNOWLEDGMENT

The authors gratefully acknowledge cooperation of H. Bassen and M. Skopec, Center for Devices and Radiological Health, FDA, Rockville, MD.

REFERENCES

[1] J. R. Le Strange, D. Byrne, K. H. Joyner, and G. L. Symons, "Interference to hearing aids by the digital mobile telephone system, global system for mobile communication," NAL, Washington, D.C., Tech. Rep. 131, May 1995.

[2] M. Skopec, "Hearing aid electromagnetic interference from digital cellular telephones," in *Proc. 18th Annu. Int. Conf. IEEE Eng. Med. Biol. Soc.*, The Netherlands, Oct. 31–Nov. 3, 1996.

[3] H. L. Bassen, "Device specific standard test method for electromagnetic interference of medical devices," in *Proc. 18th Annual Intern. Conf. IEEE Eng. Med. Biol. Soc.*, The Netherlands, Oct. 31–Nov. 3, 1996.

[4] M. Okoniewski and M. A. Stuchly, "A study of the handset antenna and human body interaction," *IEEE Trans. Microwave Theory Tech.*, vol. 44, pp. 1855–1864, Oct. 1996.

[5] V. Hombach, K. Meier, M. Burkhardt, E. Kühn, and N. Kuster, "The dependence of EM energy absorption upon human head modeling at 900 MHz," *IEEE Trans. Microwave Theory Tech.*, vol. 44, pp. 1865–1873, Oct. 1996.

[6] O. P. Gandhi, G. Lazzi, and C. M. Furse, "Electromagnetic absorption in the human head and neck for mobile telephones at 835 and 1900 MHz," *IEEE Trans. Microwave Theory Techn.*, vol. 44, pp. 1884–1897, Oct. 1996.

[7] I. G. Zubal, C. R. Harrell, E. O. Smith, Z. Rattner, G. R. Gindi, and P. H. Hoffer, "Computerized three-dimensional segmented human anatomy," *Med. Phys. Biol.*, vol. 21, pp. 299–302, 1994.

[8] K. S. Yee, "Numerical solution of initial boundary value problems involving Maxwell's equations in isotropic media," *IEEE Trans. Antennas Propagat.*, vol. 14, pp. 302–307, Apr. 1966.

[9] A. Taflove, "Computational electrodynamics: *The Finite-Difference Time-Domain Method*.Norwood, MA: Artech House, 1995.

[10] J-P. Berenger, "A perfectly matched layer for the absorption of electromagnetic waves," *J. Comput. Phys.*, vol. 114, pp. 185–200, 1994.

[11] M. Okoniewski, E. Okoniewski, and M. A. Stuchly, "Three dimensional sub-gridding algorithm for FDTD," *IEEE Antennas Propagat.*, vol. 45, pp. 422–429, Oct. 1997.

[12] C. A. Balanis, *Antenna Theory*. New York: Harper & Row, 1982.

[13] K. S. Kuntz and R. J. Luebbers, *The Finite-Difference Time Domain Method in Electromagnetics*. Boca Raton, FL: CRC Press, 1993.

Michal Okoniewski (S'88–M'89–SM'97) was born in Gdansk, Poland, in 1960. He received the M.S.E.E. and Ph.D. (with Honors) degrees from the Technical University of Gdansk, Gdansk, Poland, in 1984 and 1990, respectively.

From 1984 to 1986, he was with the Institute of Fluid Flow Machinery, Polish Academy of Sciences. From 1986 to mid-1992, he was with the Technical University of Gdansk, as an Assistant Professor. From 1992 to 1994, he was with the University of Victoria, B.C., Canada, as an NSERC International Post-Doctoral Fellow. He is currently with the University of Victoria as an Adjunct Professor. His current research interest include FDTD and other numerical methods in electromagnetics, antennas for wireless communication and methods for specific absorption rate (SAR) evaluations, interactions of electromagnetic waves with complex media, EMI, ferrite devices, and sensors for industrial applications.

Maria A. Stuchly (M'71–SM'76–F'91) received the M.Sc. degree in electrical engineering from Warsaw Technical University, Warsaw, Poland, in 1962, and the Ph.D. degree in electrical engineering from the Polish Academy of Sciences, Warsaw, Poland, in 1970.

From 1962 to 1970, she was with the Warsaw Technical University, an Institute of the Polish Academy of Sciences. After emigrating to Canada in 1970, she joined the University of Manitoba. In 1976, she joined the Bureau of Radiation and Medical Devices in Health and Welfare, Canada, as a Research Scientist. In 1978, she was with the Electrical Engineering Department, University of Ottawa, as an Adjunct Professor, and from 1990 to 1991, she was a Funding Director for the Institute of Medical Engineering. In 1992, she joined the Department of Electrical and Computer Engineering, University of Victoria, Victoria, B.C., as a Visiting Professor. Since January 1994, she has been a Professor and Industrial Research Chairholder. She was President of the Bioelectromagnetic Society (1986–1987) and Chair of the International URSI Commission K "Electromagnetics in Biology and Medicine" (1991–1993). In 1996, she was elected Vice-President of International URSI.

Dr. Stuchly currently serves at AdCom of the IEEE Biomedical Engineering Society, and is an associate editor of the IEEE TRANSACTIONS ON ANTENNAS AND PROPAGATION.